Developmental Biology 361 (2012) 125–136

Contents lists available at SciVerse ScienceDirect

Developmental Biology

journal homepage: www.elsevier.com/developmentalbiology

Influence of mesodermal *Fgf8* on the differentiation of neural crest-derived postganglionic neurons

Yiju Chen [a], Anne M. Moon [b,c], Gary O. Gaufo [a,*]

[a] Department of Biology, University of Texas at San Antonio, One UTSA Circle, San Antonio, Texas 78249, USA
[b] Department of Pediatrics, Neurobiology and Anatomy, Program in Molecular Medicine, University of Utah, Salt Lake City UT 84112, USA
[c] Department of Human Genetics, Program in Molecular Medicine, University of Utah, Salt Lake City UT 84112, USA

ARTICLE INFO

Article history:
Received for publication 24 June 2011
Revised 21 September 2011
Accepted 16 October 2011
Available online 20 October 2011

Keywords:
Cranial neural crest
Epibranchial placode
Postganglionic neurons
Fgf8
Mesoderm
Parasympathetic nervous system

ABSTRACT

The interaction between the cranial neural crest (NC) and the epibranchial placode is critical for the formation of parasympathetic and visceral sensory ganglia, respectively. However, the molecular mechanism that controls this intercellular interaction is unknown. Here we show that the spatiotemporal expression of Fibroblast growth factor 8 (Fgf8) is strategically poised to control this cellular relationship. A global reduction of *Fgf8* in hypomorph embryos leads to an early loss of placode-derived sensory ganglia and reduced number of NC-derived postganglionic (PG) neurons. The latter finding is associated with the early loss of NC cells by apoptosis. This loss occurs concurrent with the interaction between the NC and placode-derived ganglia. Conditional knockout of *Fgf8* in the anterior mesoderm shows that this tissue source of Fgf8 has a specific influence on the formation of PG neurons. Unlike the global reduction of *Fgf8*, mesodermal loss of *Fgf8* leads to a deficiency in PG neurons that is independent of NC apoptosis or defects in placode-derived ganglia. We further examined the differentiation of PG precursors by using a quantitative approach to measure the intensity of Phox2b, a PG neuronal determinant. We found reduced numbers and immature state of PG precursors emerging from the placode-derived ganglia en route to their terminal target areas. Our findings support the view that global expression of Fgf8 is required for early NC survival and differentiation of placode-derived sensory neurons, and reveal a novel role for mesodermal Fgf8 on the early differentiation of the NC along the parasympathetic PG lineage.

Introduction

The complexity of the cranial division of the peripheral nervous system manifests from the interaction between the pluripotent neural crest (NC) and the myriad of precursor cells in the head, neck, and thoracic-abdominal compartments of the body (Begbie and Graham, 2001; Begbie et al., 1999; Bogni et al., 2008; Chen et al., 2011; Enomoto et al., 1998, 2000; Gammill et al., 2006, 2007; Heuckeroth et al., 1999; Le Douarin et al., 2004; Schwarz et al., 2008; Shiau et al., 2008; Uesaka et al., 2007; Yan et al., 2004; Young et al., 2004). Cranial NC cells delaminate from the dorsal edge of the midbrain and hindbrain, and migrate to the periphery, where they differentiate into a variety of cell types, including mesenchyme, melanocytes, different regions of the heart, and ganglia that make up the various neuronal and glial components of the peripheral and enteric nervous systems (Creuzet et al., 2005; Le Douarin et al., 2004; Noden and Trainor, 2005). The functional integration of NC cells and associated peripheral cells is dependent upon their position along the anterior–posterior (AP) axis (Lumsden and Krumlauf, 1996; Lumsden et al., 1991; Trainor and Krumlauf, 2000, 2001). For instance, at the midbrain level, the reciprocal interaction between midbrain NC cells and adjacent cells derived from the ophthalmic placode is critical for the formation of the trigeminal ganglion (Artinger et al., 1998; Baker and Bronner-Fraser, 2001; Baker et al., 1999; Hamburger, 1961; McCabe and Bronner-Fraser, 2008; Shiau and Bronner-Fraser, 2009; Shiau et al., 2008; Stark et al., 1997). At the posterior end of the developing brainstem, the interaction between caudal rhombomere (r)-derived NC cells and the cellular environment of the gut is critical for the formation of enteric neurons (Bogni et al., 2008). These examples illustrate the importance of peripheral tissues in determining the fate of cranial NC cells.

Recent findings have shown that the formation of complementary parasympathetic and visceral sensory ganglia of the VIIth and IXth cranial nerves is dependent on the reciprocal interaction between cranial NC- and epibranchial placode-derived neurons (Chen et al., 2011; Coppola et al., 2010; Takano-Maruyama et al., 2010). Each pair of complementary ganglia contributes to a simple 3-neuron polysynaptic reflex circuit. Sensory information from visceral tissues in the head, neck, thoracic, and abdominal regions of the body is detected by neurons contained within epibranchial placode-derived

* Corresponding author. Fax: +1 210 458 5658.
E-mail address: gary.gaufo@utsa.edu (G.O. Gaufo).

0012-1606/$ – see front matter © 2011 Elsevier Inc. All rights reserved.
doi:10.1016/j.ydbio.2011.10.019

sensory ganglia. Central processes of placode-derived sensory neurons project directly or indirectly to preganglionic motor neurons in the midbrain and hindbrain, which in turn, innervate peripheral parasympathetic postganglionic (PG) neurons. PG neurons represent the final pathway that ultimately regulates the function of visceral target tissues (Takano-Maruyama et al., 2010). This visceral sensorimotor reflex circuit therefore controls the secretomotor activity of pre- and post-ganglionic (PG) neurons as a consequence of visceral input from placode-derived visceral sensory ganglia. Interestingly, this functional relationship manifests from a developmental interaction in which the placode-derived sensory ganglia controls the axon pattern of preganglionic neurons and the formation of PG neurons (Coppola et al., 2010; Takano-Maruyama et al., 2010).

The various epibranchial placodes give rise to visceral sensory neurons of the geniculate, petrosal, and nodose ganglia (Baker and Bronner-Fraser, 2001; Begbie et al., 2002; Schlosser, 2010). Visceral sensory precursors delaminate from epibranchial placodes located at the clefts of the second, third, and fourth branchial arches, and migrate toward the hindbrain to form visceral sensory ganglia associated with VIIth, IXth, and Xth cranial nerves respectively. The migration of each pair of ganglia is facilitated by adjacent rhombomere-derived NC cells (Begbie and Graham, 2001). As noted above, the epibranchial placode-derived sensory ganglia function as critical intermediate targets through which the NC fated for the parasympathetic PG lineage and axons of preganglionic neurons navigate through prior to reaching their distant terminal target sites (Takano-Maruyama et al., 2010). Although the cellular interaction is critical for the formation of this visceral sensorimotor circuit (Chen et al., 2011; Coppola et al., 2010; Takano-Maruyama et al., 2010), the molecular contribution from surrounding tissues in this developmental process is unknown.

In the vertebrate head, Fibroblast growth factors (Fgfs) are key signaling molecules involved in cell survival, proliferation and differentiation (Mason, 2007). In particular, Fgf8 is expressed in the ectoderm adjacent to developing epibranchial placode-derived sensory ganglia, the anterior mesoderm, and the endoderm (Ladher et al., 2005; Macatee et al., 2003; Nechiporuk et al., 2005, 2007; Park et al., 2006; Trainor et al., 2002a) (Supplementary Fig. S1). *Fgf8* has been shown to be required for mesenchymal cell survival and branchial arch morphogenesis (Trumpp et al., 1999). Additionally, Fgf8 signals from pharyngeal mesoderm and endoderm have been shown to be critical for cardiac NC cell proliferation, and survival of cardiac precursors in the second heart field during cardiac outflow tract development (Abu-Issa et al., 2002; Frank et al., 2002; Park et al., 2006; Watanabe et al., 2010). Fgf8 has also been demonstrated to be chemotactic for chick cardiac NC through Fgf receptors (Fgfrs) 1 and 3 and the MAPK/ERK signaling pathway (Sato et al., 2011). In Xenopus, Fgf8 regulates NC delamination and migration through the transcription factors msx1, pax3 and slug (Monsoro-Burq et al., 2005). Furthermore, morpholino knockdown and gain-of-function studies in zebrafish show that endoderm-derived Fgf3 is necessary and sufficient to control neurogenesis in the epibranchial placode (Nechiporuk et al., 2005). Together, these findings suggest that Fgf signals are strategically expressed in various tissues in the vertebrate head to coordinate the formation of NC and epibranchial placode-derived parasympathetic and visceral sensory ganglia, respectively.

In this study, we use the VIIth and IXth parasympathetic cranial nerves as models to test both global and tissue-specific requirements for Fgf8 on the formation of complementary parasympathetic and visceral sensory ganglia associated with these cranial nerves. We show that the formation of PG neurons that comprise the various parasympathetic ganglia, specifically the sphenopalatine (Spg), submandibular (Smg), and otic (Og) ganglia, is dependent on *Fgf8*. *Fgf8* deficiency leads a defect in the early differentiation of epibranchial placode-derived sensory ganglia, and NC apoptosis associated with PG precursors. These defects are associated with reduction of the Spg, Smg, and Og. To further define how *Fgf8* regulates the formation of PG neurons, conditional ablation of *Fgf8* in the anterior mesoderm was generated (Park et al., 2006). Again, a reduction of PG neuronal formation was observed. However, the tissue-restricted loss of mesodermal *Fgf8* does not lead to NC apoptosis, as observed with the global reduction of *Fgf8*. By using a novel approach to quantify protein intensity of Phox2b, a PG neuronal determinant (Pattyn et al., 1999), we found a defect in the early differentiation of PG precursors in mesoderm-ablated *Fgf8* embryos compared to controls. These data suggest that Fgf8 via the mesoderm acts non-cell autonomously on the cranial NC to affect an early stage of PG neuronal differentiation.

Material and methods

Mouse strains

The *Fgf8* hypomorph, conditional, and *GFP* reporter alleles, and *AP2α*$^{Ires\text{-}Cre/+}$ and *MesP1*$^{Cre/+}$ drivers have been described (Frank et al., 2002; Macatee et al., 2003; Moon and Capecchi, 2000; Park et al., 2006; Saga et al., 1996).

Immunohistochemistry

Embryos (e9.5-e12.5) were fixed in 4% paraformaldehyde/PBS for 30 min, and then cryoprotected in a sequential series of 15% sucrose/PBS overnight, and 30% sucrose/PBS 3–4 h. Embryos were then embedded in OCT compound-filled molds (Tissue Tek), and then frozen rapidly. Cryosections were cut sagitally for confocal microscopy (12 μm) and cell counting (16 μm), and mounted on charged glass slides (Fisher). Sections were blocked in PBST (phosphate-buffered saline with 1% Triton X-100) containing 10% skimmed milk and 10% normal goat serum for 5 min at room temperature. Primary antibodies were diluted in PBST containing 5% skimmed milk and 5% normal goat serum, and applied to the sections overnight at 4 °C. The following primary antibodies were used for the present study: rabbit polyclonal anti-Phox2b antibody (1:40,000; generated in our laboratory), neuron-specific class III β-tubulin marker, TuJ1 (1:2500, Covance); rabbit anti phosphohistone H3 (PHH3, 1:500, Cell Signaling); mouse anti-Islet1/2 (1:100, DSHB); mouse anti-neurofilament (1:200, DSHB); mouse anti-AP-2 alpha (AP2, 1:50, DSHB); and mouse anti-Sox10 (1:150, a gift from D. Anderson). TOTO-3 was used as nuclear marker (1:1000, Molecular Probes). The sections were then washed with PBST, and Alexa fluorescence-conjugated secondary antibodies (1:500 or 1:1000, Molecular probes) were applied for 1 h at room temperature in a dark, humidified chamber. After washing, 50% glycerol/PBST was added to the sections and cover slips applied. 3D fluorescent image Z-stacks were subsequently taken by LSM5 PASCAL Laser Scanning Confocal Imaging System.

TUNEL assay

Apoptotic cells were detected by the TUNEL assay (*In Situ* Cell Death Detection Kit, TMR red; Roche Applied Science). The TUNEL assay was performed according to the manufacturer's protocol. Cryosections were prepared as above. After application of primary antibodies overnight, slides were washed with PBST. Slides were then incubated with the TUNEL reaction mixture for 1 h at 37 °C in a dark, humidified chamber. After washing, the slides were mounted with 50% glycerol/PBST, and 3D fluorescent image Z-stacks were taken by using the LSM5 PASCAL Confocal Imaging System.

Cell counting, cell intensity and statistics

After deconvolving the 3D images, the immunolabeled cells were counted and analyzed by the IMARIS software (Version 6.1.5, Bitplane

Scientific Software). First, the co-localized channels of Phox2b/TOTO-3 or Phox2b/Islet1 were built, and the diameter of 4 μm was used to count single cells ("spot" function in IMARIS). The total cell number for the Spg, Smg, Og, VIIg, or IXg was summed, and at least three embryos were counted for each ganglion. A paired student *t*-test was used to measure statistical significance. Second, the "region grow" function in IMARIS was applied to generate shells to cover each single Phox2b$^+$/Sox10$^+$ cell in the entire field. The mean intensity of each cell was then used to normalize the total number per side. The R program (http://www.r-project.org/) was used to determine the relative density plot.

Results

Formation of cranial parasympathetic ganglia and their non-neuronal targets requires Fgf8

In contrast to the sympathetic chain ganglia, the parasympathetic ganglia are located close to or embedded within their non-neuronal targets (Kandel et al., 2000). Previous studies have shown that *Fgf8* is essential for the formation of the non-neuronal targets of the cranial parasympathetic ganglia, such as cardiovascular, lung, and salivary gland tissues (Al-Hadithi and Mitchell, 1987; Frank et al., 2002; Jaskoll et al., 2005; Yu et al., 2010). It also appears that Fgf8 is strategically expressed in the head ectodermal region where the epibranchial placode-derived sensory ganglia originate, and placodal and NC cells interact (Begbie and Graham, 2001; Macatee et al., 2003; Mason, 2007; Park et al., 2006; Takano-Maruyama et al., 2010; Trainor et al., 2002a). To examine this relationship, we analyzed sagittal sections of e9.5 mouse embryos harboring an Fgf8-GFP reporter (Macatee et al., 2003). We found that Fgf8-GFP is expressed in the ectodermal region containing the complementary location of Sox10$^+$ r4 and r6 NC cells and delaminating Phox2a$^+$ cells that contribute to the placode-derived geniculate and petrosal ganglia (Supplementary Fig. S1). This led us to reason that the complementary NC-derived parasympathetic and placode-derived visceral sensory ganglia could be affected directly or indirectly by eliminating *Fgf8* function.

To address this, we first examined the NC-derived parasympathetic Spg, Smg, and Og in *Fgf8* mutant embryos. These ganglia innervate the nasal mucosa, submandibular and parotid glands, respectively (Kandel et al., 2000). Specifically, we analyzed *Fgf8* hypomorph embryos (*Fgf8*$^{H/-}$) to determine whether global expression of *Fgf8* is required for the development of the Spg, Smg, and Og. The *Fgf8*$^{H/-}$ embryo has the advantage of bypassing the early lethality associated with germline ablation of *Fgf8*, while producing dramatically less *Fgf8* as compared to control littermates (Frank et al., 2002). Due to the critical cell-autonomous function of the transcription factor Phox2b in PG neuronal formation (Coppola et al., 2010; Pattyn et al., 1999), we used Phox2b immunolabeling to identify PG neurons. In e12.5 sagittal sections of control embryos, we visualized Phox2b, and Tuj1 (pan neural marker), and TOTO-3 (cell nucleus marker). The cigar-shaped cluster of Phox2b$^+$ PG neurons of the Spg is closely associated with the ophthalmic vein (Fig. 1A). The total number of Phox2b$^+$ cells in the Spg was significantly reduced by 79.2% in *Fgf8*$^{H/-}$ embryos compared to control littermates (Figs. 1A–C; control, 4326 ± 523; *Fgf8*$^{H/-}$, 899 ± 289; n = 3, $p < 0.05$). The Tuj1$^+$ fibers can be found in both control and *Fgf8*$^{H/-}$ embryos, and are likely derived from sensory neurons of the maxillary division of the trigeminal ganglion (Figs. 1A, B). A 90.8% reduction of Phox2b$^+$ PG neurons was also observed in the Smg of *Fgf8*$^{H/-}$ embryos (Figs. 1D–F; control, 1658 ± 63; *Fgf8*$^{H/-}$, 153 ± 61; n = 3, $p < 0.005$). The target of the Smg, the submandibular gland (dotted line), is absent in *Fgf8*$^{H/-}$ embryos (Figs. 1D, E) as previously reported (Jaskoll et al., 2004). Furthermore, the total number of Phox2b$^+$ PG neurons in the Og was significantly reduced by 78.3% in *Fgf8*$^{H/-}$ embryos compared to control littermates (Figs. 1G–I; control, 1553 ± 87; *Fgf8*$^{H/-}$, 337 ± 211; n = 4, $p < 0.05$; note the neurons of the Og are positive for Phox2b, whereas those for the VIIg are positive for both Phox2b and Isl1). These results suggest that *Fgf8* is involved in the formation of NC-derived PG neurons of the Spg, Smg and Og. Moreover, these ganglia arise from different rhombomeres, thereby implicating *Fgf8* in controlling multiple NC populations along the AP axis (Chen et al., 2011; D'Amico-Martel and Noden, 1983; Takano-Maruyama et al., 2010; Yang et al., 2008).

Global reduction of Fgf8 leads to apoptosis of NC and defect in differentiation of placodal ganglia

To define when *Fgf8* is required for PG neuronal development, we analyzed control and *Fgf8*$^{H/-}$ embryos at e9.5. At this stage, the NC-derived PG precursors have yet to reach their non-neuronal targets, but are engaged with the epibranchial placode-derived sensory ganglia (Chen et al., 2011; Takano-Maruyama et al., 2010). The survival and differentiation of PG precursors have been shown to depend on their early interaction with the epibranchial placode-derived visceral sensory ganglia (Coppola et al., 2010; Takano-Maruyama et al., 2010). To determine whether *Fgf8* is required for this early interaction and whether the loss of NC cells is a consequence of apoptosis prior to their commitment to the PG lineage, we evaluated the status of NC cells located between r4 and the complementary epibranchial placode-derived geniculate ganglion in ba2. In sagittal sections, we observed less placode-derived geniculate precursors delaminating at the cleft of ba2 and a dramatic increase in TUNEL labeling in *Fgf8*$^{H/-}$ embryos compared to control littermates (Figs. 2A–F). Specifically, the stream of TUNEL labeling was observed in the region where Sox10$^+$ r4 NC and Phox2b$^+$ placode geniculate-derived neuronal precursors were normally engaged. This phenotype was also observed in the ba3 region where r6 NC- and petrosal placode-derived neuronal precursors are normally engaged (Figs. 2G, H). Although we found a dramatic increase in TUNEL labeling associated with the NC and placode-derived ganglia, few Sox10$^+$ and Phox2b$^+$ cells were labeled with TUNEL. This suggests that the majority of TUNEL labeling is a residue of fragmented DNA from cells that presumably expressed Phox2b and/or Sox10. However, we cannot exclude the possibility that apoptotic mesenchymal, placodal, or other cell types contribute to the overall TUNEL labeling in this area of *Fgf8*$^{H/-}$ embryos.

We further explored how the global reduction of Fgf8 affects the development of the epibranchial placode-derived ganglia. Statistical analysis showed that the total number of Phox2b$^+$/Isl1$^+$ neurons in the placode-derived geniculate ganglion was dramatically reduced in *Fgf8*$^{H/-}$ embryos compared to control littermates at e9.5 (Figs. 2I-K; control, 325 ± 90; *Fgf8*$^{H/-}$, 86 ± 11; n = 4, $p = 0.06$). It is interesting to note that in contrast to *Fgf8*$^{H/-}$ embryos, the number of Phox2b$^+$/Isl1$^+$ neurons in the placode-derived geniculate ganglion varied dramatically among control embryos. Although this difference likely reflects the size and slight age difference among e9.5 control embryos, the variability of Phox2b$^+$/Isl1$^+$ neurons was very small among *Fgf8*$^{H/-}$ embryos. However, by e12.5 the total number of Phox2b$^+$/Isl1$^+$ neurons in the placode-derived geniculate ganglion was not statistically different between control and *Fgf8*$^{H/-}$ embryos (Figs. 2L-N; control, 1406 ± 136; *Fgf8*$^{H/-}$, 1416 ± 205; n = 3, $p = 0.9$). Global reduction of *Fgf8* therefore has an early effect in the development of the placode-derived geniculate ganglion, but not at later stages. However, we cannot be certain that this conclusion also extends to the placode-derived petrosal ganglion. At e12.5, the petrosal and nodose ganglia were fused in many control and *Fgf8*$^{H/-}$ embryos. This made it difficult to perform cell counting for individual ganglion, and thus determine the effect of the global loss of Fgf8 in the formation of the placode-derived petrosal ganglion.

Our findings thus far suggest that the global reduction of Fgf8 may affect two interrelated events that lead to the reduction of PG neurons in the *Fgf8*$^{H/-}$ embryo. First, the early defect in the placode-derived geniculate and petrosal ganglia, either through programmed cell death and/or delay in differentiation, may indirectly affect the survival of NC cells fated for the PG lineage (Coppola et al., 2010; Takano-Maruyama et al., 2010). Second, the increase in apoptosis among r4 and r6 NC cells may

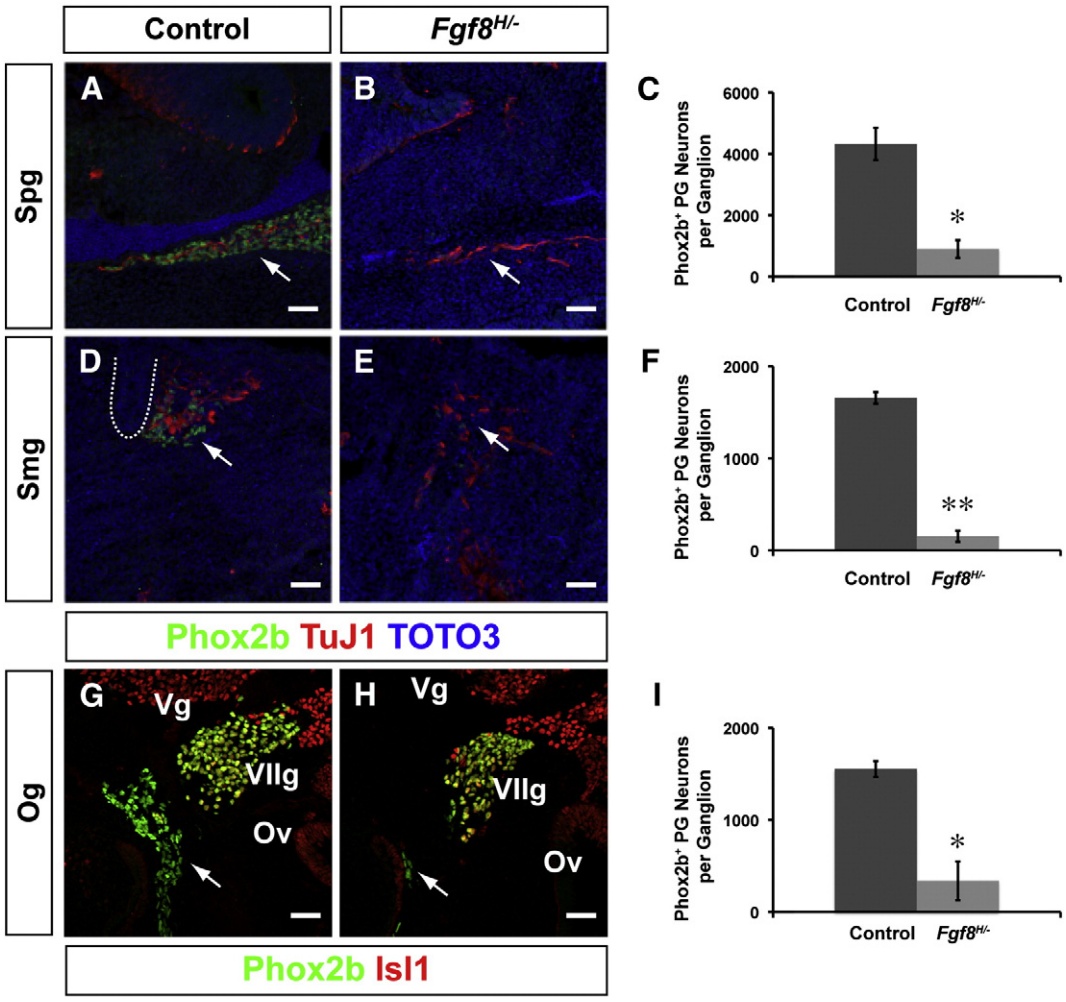

Fig. 1. *Fgf8* is required for the formation of parasympathetic postganglionic neurons. (A–C) Sagittal sections of e12.5 control and *Fgf8* hypomorph embryos through the sphenopalatine ganglion (Spg) immunolabeled for Phox2b (green), TuJ1 (red), and TOTO3 (blue). The total number of Phox2b$^+$ postganglionic (PG) neurons per ganglion was counted in control (n = 3) and *Fgf8* hypomorph (n = 3) embryos. The number of PG neurons was significantly reduced in *Fgf8* hypomorph embryos compared to control embryos ($^*p<0.05$). (D–F) Sagittal sections of e12.5 control and *Fgf8* hypomorph embryos through the submandibular ganglion (Smg) immunolabeled for Phox2b (green), TuJ1 (red), and TOTO3 (blue). The total number of Phox2b$^+$ PG neurons per ganglion was counted in control (n = 3) and *Fgf8* hypomorph (n = 3) embryos. The number of PG neurons was significantly reduced in *Fgf8* hypomorph embryos compared to control embryos ($^{**}p<0.005$). The dotted outline in panel D shows the location of the submandibular gland in the control embryo, which is missing in the *Fgf8* hypomorph embryo (panel E). (G–I) Sagittal sections of e12.5 control and *Fgf8* hypomorph embryos through the otic ganglion (Og) immunolabeled for Phox2b (green) and Isl1 (red). The total number of Phox2b$^+$ PG neurons was counted in control (n = 4) and *Fgf8* (n = 4) hypomorph embryos. The number of PG neurons was significantly reduced in *Fgf8* hypomorph compared to control embryos ($^*p<0.05$). Bars represent standard error. Arrows indicate the location of the Spg, Smg and Og. Abbreviations: *Fgf8*$^{H/-}$, *Fgf8* hypomorph; Vg, trigeminal ganglion; Ov, otic vesicle. Scale bar = 50 μm.

reflect a direct requirement for Fgf8 on NC survival (Park et al., 2006; Watanabe et al., 2010), which in turn may lead to a reduction in NC-derived PG neurons. Experiments to ablate *Fgf8* function in a tissue-specific manner could begin to address some of these issues. Based on the expression of Fgf8-GFP in the ectoderm (Supplementary Fig. S1), we reasoned that the loss of ectodermal *Fgf8* could potentially disrupt a paracrine signal required for the early survival and/or differentiation of placode- and NC-derived neuronal precursors. Surprisingly, conditional ablation of *Fgf8* in the ectoderm (*Fgf8*$^{flox/flox}$;*AP2*$^{Ires\text{-}Cre/+}$) did not affect the early differentiation of placode-derived ganglia or survival of NC cells at the ba2/r4 and ba3/r6 levels of e9.5 embryos (Supplementary Fig. S2). This suggests that another tissue source of Fgf8 or the combination of Fgf8 from multiple sources may contribute to the early differentiation and/or survival of placode-derived ganglia and NC cells.

Mesodermal Fgf8 contributes to the formation of cranial parasympathetic ganglia

Previous findings in the mouse and zebrafish indicate that mesodermal Fgf8 influences the development of the NC and the epibranchial placode (Nechiporuk et al., 2007; Park et al., 2006; Watanabe et al., 2010). In the mouse, mesoderm-derived Fgf8 is required for the proper development of the outflow tract and the pharyngeal arch arteries (Park et al., 2006; Watanabe et al., 2010). In combination with a loss of one allele of *Fgf10*, a deficiency in mesodermal *Fgf8* leads to apoptosis of the cardiac NC population that gives rise to the outflow tract of the heart (Watanabe et al., 2010). In zebrafish, the combination of mesoderm-derived Fgf8 and Fgf3 is required for induction of the epibranchial placodes (Nechiporuk et al., 2007). Based on these findings, it is possible that mesoderm-derived Fgf8 may affect the development of the more rostral (relative to cardiac) NC populations that give rise to PG neurons of the Spg, Smg, and Og.

To test this possibility, we employed the *MesP1*$^{Cre/+}$ to conditionally knockout *Fgf8* in the anterior mesoderm starting at e6.5 (Macatee et al., 2003; Saga et al., 1996). We then analyzed the formation of PG neurons in control and *Fgf8*$^{flox/flox}$;*MesP1*$^{Cre/+}$ (referred hereafter as *Fgf8*^{CKO}) embryos at e12.5. Again, sagittal sections were immunolabeled for Phox2b to identify NC-derived PG neurons of the Spg, Smg, and Og, and in combination with Isl1 to identify the placode-derived ganglia (Figs. 3A–I). The total number of r4 NC-derived Phox2b$^+$ PG neurons in the Spg shows a

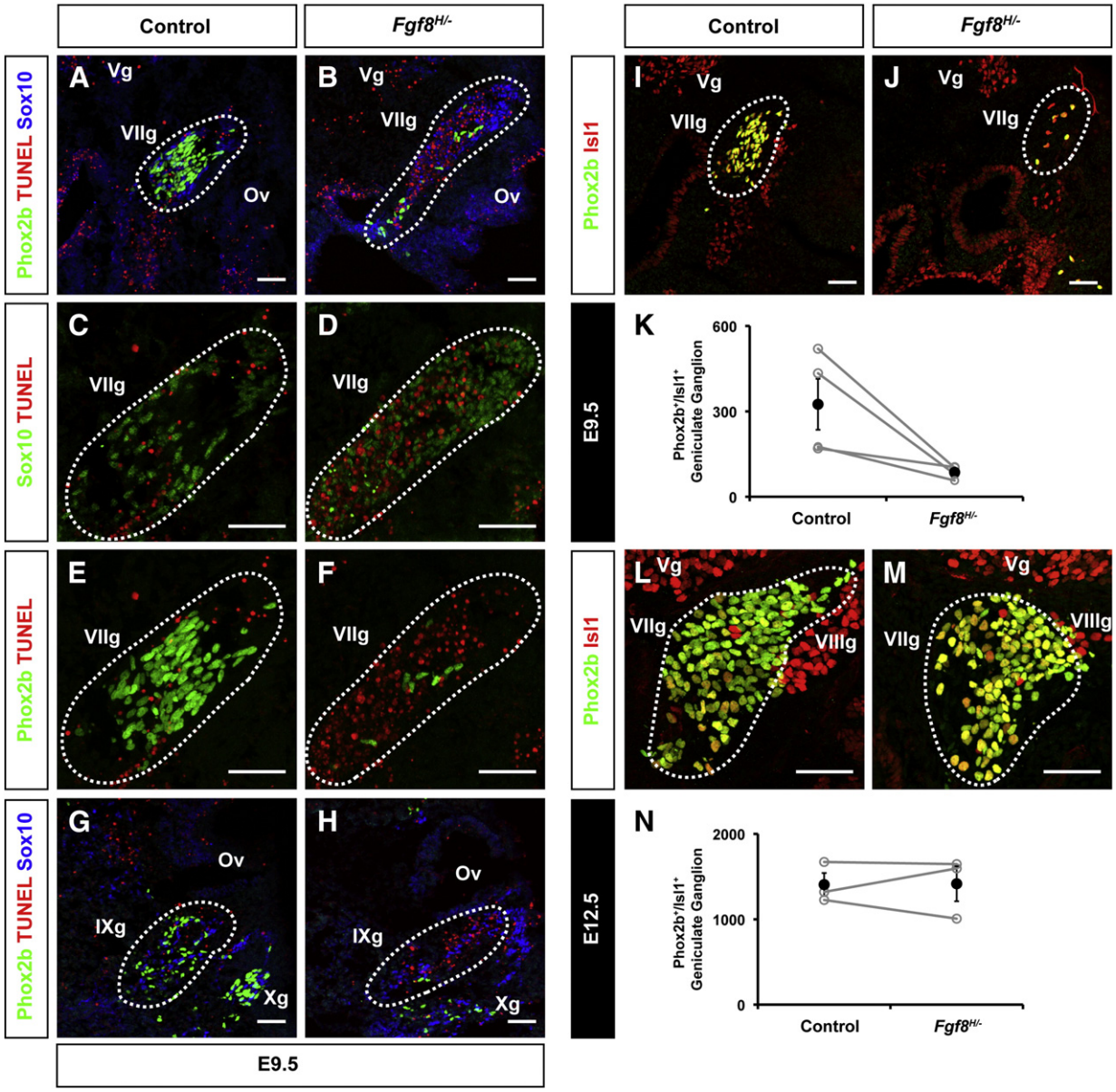

Fig. 2. Loss of *Fgf8* leads to increased apoptosis associated with r4- and r6-derived neural crest cells and placode-derived ganglia. (A–B) Sagittal sections of e9.5 control (n = 4) and *Fgf8* hypomorph (n = 4) embryos through the geniculate ganglion immunolabeled for Phox2b (green) and Sox10 (blue), and assayed for TUNEL (red) (20X). (C–D) Sagittal sections of e9.5 control (n = 4) and *Fgf8* hypomorph (n = 4) embryos through the geniculate ganglion immunolabeled for Sox10 (green) and assayed for TUNEL (red) (40X). (E–F) Sagittal sections of e9.5 control (n = 4) and *Fgf8* hypomorph (n = 4) embryos through the geniculate ganglion immunolabeled for Phox2b (green) and assayed for TUNEL (red) (40X). (G–H) Sagittal sections of e9.5 control (n = 4) and *Fgf8* hypomorph (n = 4) embryos through the petrosal ganglion immunolabeled for Phox2b (green) and Sox10 (blue), and assayed for TUNEL (red) (20X). (I, J) Sagittal sections of e9.5 control and *Fgf8* hypomorph embryos through the geniculate ganglion immunolabeled for Phox2b (green), and Isl1 (red). Phox2b/Isl1-double positive cells indicate the geniculate ganglion (VIIg), and Isl1-single positive cells indicate the trigeminal (Vg) and vestibulocochlear (VIIIg) ganglia. (K) The total number of Phox2b/Isl1-double positive cells in the geniculate ganglion was counted in control (n = 4) and *Fgf8* hypomorph (n = 4) embryos. Each gray line represents one pair of control and $Fgf8^{H/-}$ littermate. The black dot is the mean value of the whole set. The error bar indicates standard error mean. Note the relatively large variance in control versus Fgf8 hypomorph embryos. This indicates a requirement for Fgf8 in the early differentiation of neurons contributing to the geniculate ganglion. (L–M) Sagittal sections of e12.5 control and *Fgf8* hypomorph embryos through the geniculate ganglion immunolabeled for Phox2b (green), and Isl1 (red). Phox2b/Isl1-double positive cells indicate the geniculate ganglion (VIIg), and Isl1-single positive cells indicate the trigeminal (Vg) and vestibulocochlear (VIIIg) ganglia. (N) The total number of Phox2b/Isl1-double positive cells in the geniculate ganglion was counted in control (n = 3) and *Fgf8* hypomorph (n = 3) embryos. Each gray line represents one pair of control and $Fgf8^{H/-}$ littermate. The black dot is the mean value of the whole set. The error bar indicates standard error mean. By e12.5, the difference in number of Phox2b/Isl1-double positive neurons in the geniculate ganglion of control versus Fgf8 hypomorph embryos was not statistically significant. Dotted outlines in panels A–H show rhombomere-specific NC streams associated with the adjacent placode-derived ganglion (panels A–F, r4 NC stream; panels G-H, r6 NC stream). Note that in e9.5 *Fgf8* hypomorph embryos the VIIg (geniculate) and IXg (petrosal) ganglia were reduced, and apoptosis was associated with rhombomere-specific NC cells and the adjacent placode-derived ganglion. Abbreviations: $Fgf8^{H/-}$, *Fgf8* hypomorph; Vg, trigeminal ganglion; Xg, nodose ganglion; Ov, otic vesicle. Scale bar = 50 μm.

23.4% reduction in $Fgf8^{CKO}$ embryos compared to control littermates (Figs. 3A–C; control, 5831 ± 231; $Fgf8^{CKO}$, 4465 ± 573; n = 3, $p = 0.067$). Similarly, we observed a 30.6% reduction of r4 NC-derived PG neurons in the Smg (Figs. 3D-F; control, 1960 ± 121; $Fgf8^{CKO}$, 1361 ± 114; n = 3, $p < 0.05$). Finally, a 24.7% reduction of r6 NC-derived PG neurons was observed in the Og of $Fgf8^{CKO}$ embryos compared to control embryos (Figs. 3G–I; control, 1945 ± 76; $Fgf8^{CKO}$, 1464 ± 97; n = 3, $p < 0.05$). Compared to the global loss of *Fgf8* in $Fgf8^{H/-}$ embryos, these results define a specific contribution of mesoderm *Fgf8* during the early formation of the NC-derived Spg, Smg, and Og. Consistent with the severe reduction in

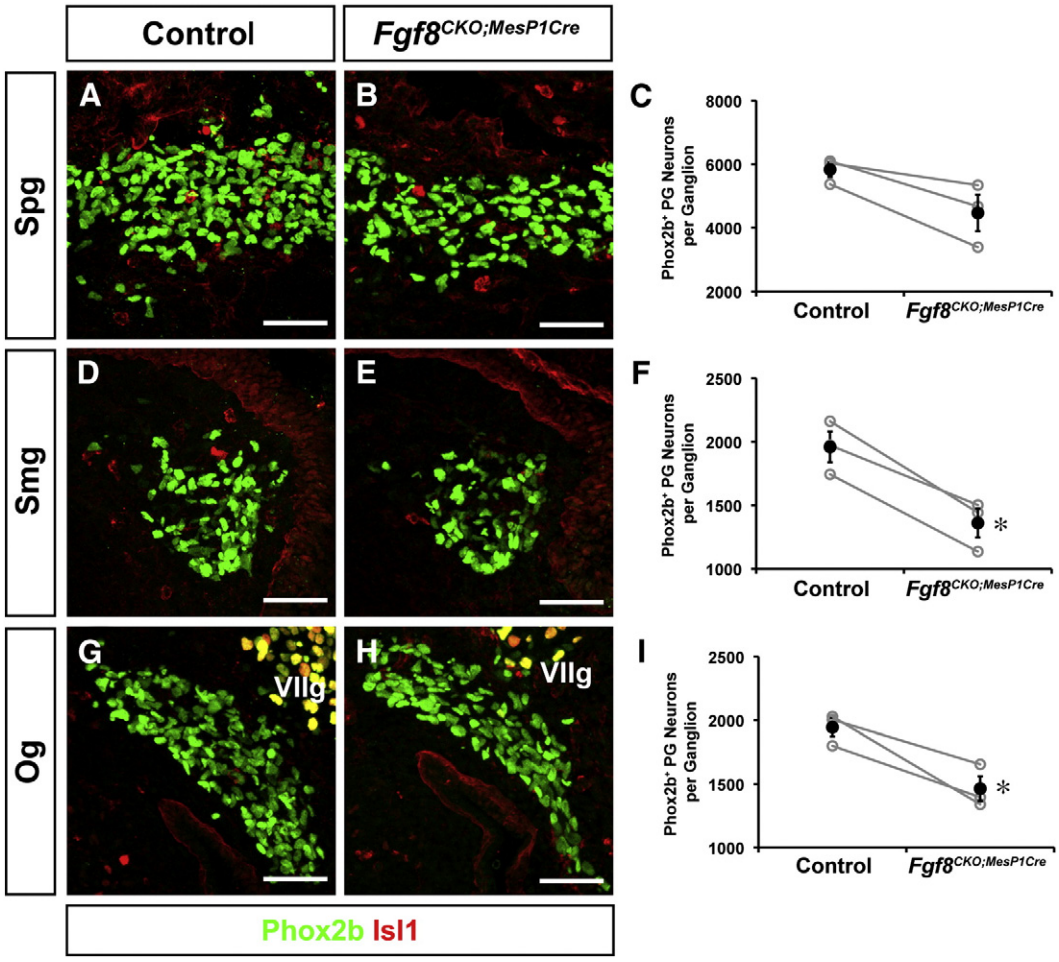

Fig. 3. Mesodermal *Fgf8* contributes to the formation of cranial parasympathetic ganglia. (A–B, D–E, G–H) Sagittal sections through the sphenopalatine (Spg), submandibular (Smg), and otic (Og) ganglia of e12.5 control and $Fgf8^{CKO};MesP1^{Cre/+}$ littermate embryos immunolabeled for Phox2b (green) and Isl1 (red). (C, F, I) Quantitative analysis of the total number of $Phox2b^{+}$ PG neurons in the Spg, Smg, and Og in control (n = 3) and $Fgf8^{CKO};MesP1^{Cre/+}$ (n = 3) embryos (* $p<0.05$). Each gray line represents one pair of control and $Fgf8^{CKO};MesP1^{Cre/+}$ littermate. The black dot is the mean value of the whole set (n = 3). The error bar indicates standard error mean. The Spg, Smg, and Og were respectively reduced by 23% ($p = 0.067$), 31% (*$p<0.05$), and 25% (*$p<0.05$) in $Fgf8^{CKO};MesP1^{Cre/+}$ embryos compared to control embryos. Note that the Spg, Smg, and Og are defined by the expression of Phox2b, and the geniculate ganglion (VIIg) is defined by the expression of both Phox2b and Isl1. Abbreviations: VIIg, geniculate ganglion; CKO, conditional knockout. Scale bar = 50 μm.

PG numbers in *Fgf8* hypomorph embryos, the partial reduction of PG neurons in mesoderm *Fgf8*-deficient embryos suggests that other tissue sources contribute to the overall formation of the Spg, Smg and Og.

Mesodermal Fgf8 does not influence the survival or formation of neural crest and epibranchial placode-derived ganglia

We have shown that r4-derived NC cells migrate through the adjacent epibranchial placode-derived geniculate ganglion en route to their terminal target sites (Takano-Maruyama et al., 2010). Within the geniculate ganglion, a population of NC cells begins to differentiate into PG precursors starting at about e9.5. Using a Fgf8-GFP reporter in the mouse, it was shown that Fgf8 is expressed in the splanchnic, dorsal, and paraxial mesoderm areas between the 3 to 6 somite stages (Ladher et al., 2005). This mesodermal expression of Fgf8 is required for the survival of cardiac NC cells (Park et al., 2006; Watanabe et al., 2010). These findings suggest that the early mesodermal expression of Fgf8 may also be important for setting up the environment for survival, proliferation, migration, and/or differentiation for the more anterior NC cells fated for the PG lineage of the Spg, Smg, and Og.

To determine whether the loss of PG neurons in $Fgf8^{CKO}$ embryos is a consequence of an early defect in the NC or epibranchial placode-derived ganglia, we analyzed e9.5 embryos. We first examined apoptosis and proliferation in the $Sox10^{+}/AP2^{+}$ NC streams that arise from r4 and r6 (Figs. 4 and 5), both of which were dramatically affected in *Fgf8* hypomorph embryos. We evaluated cell apoptosis by the TUNEL assay. No significant difference in the number or location of TUNEL-positive cells and cellular debris were observed in either r4- or r6-derived NC streams between control and $Fgf8^{CKO}$ embryos (Figs. 4A–E; 5A, B; the NC stream and associated $Phox2b^{+}$ placode-derived ganglion are circumscribed by the dotted outline). We also evaluated cell proliferation by immunolabeling for the mitosis marker Phospho-Histone H3 (PHH3) and the proliferation marker Ki67. We found no difference in PHH and Ki67 associated with either r4 or r6-derived PG precursors between control and $Fgf8^{CKO}$ embryos (Figs. 4F–K; 5C–F). We next tested whether the loss of mesodermal *Fgf8* affects the early differentiation of $Phox2b^{+}$ placode-derived sensory ganglia as seen in e9.5 *Fgf8* hypomorph embryos (Fig. 2). We evaluated the total number of $Phox2b^{+}$ cells in the geniculate (VIIg) and petrosal (IXg) ganglia of control and $Fgf8^{CKO}$ embryos. In contrast to *Fgf8* hypomorph embryos, the loss of mesodermal *Fgf8* did not significantly affect the size (numbers) or location of these epibranchial placode-derived ganglia (Figs. 6A–C, VIIg; 6D–E, IXg). These results indicate that the reduction of PG neurons in the absence of mesodermal *Fgf8* is not a consequence of early defects in cell survival or proliferation among NC-derived PG precursors, or indirectly via the epibranchial placode-derived sensory ganglia. Analysis of e12.5 $Fgf8^{CKO}$ embryos revealed

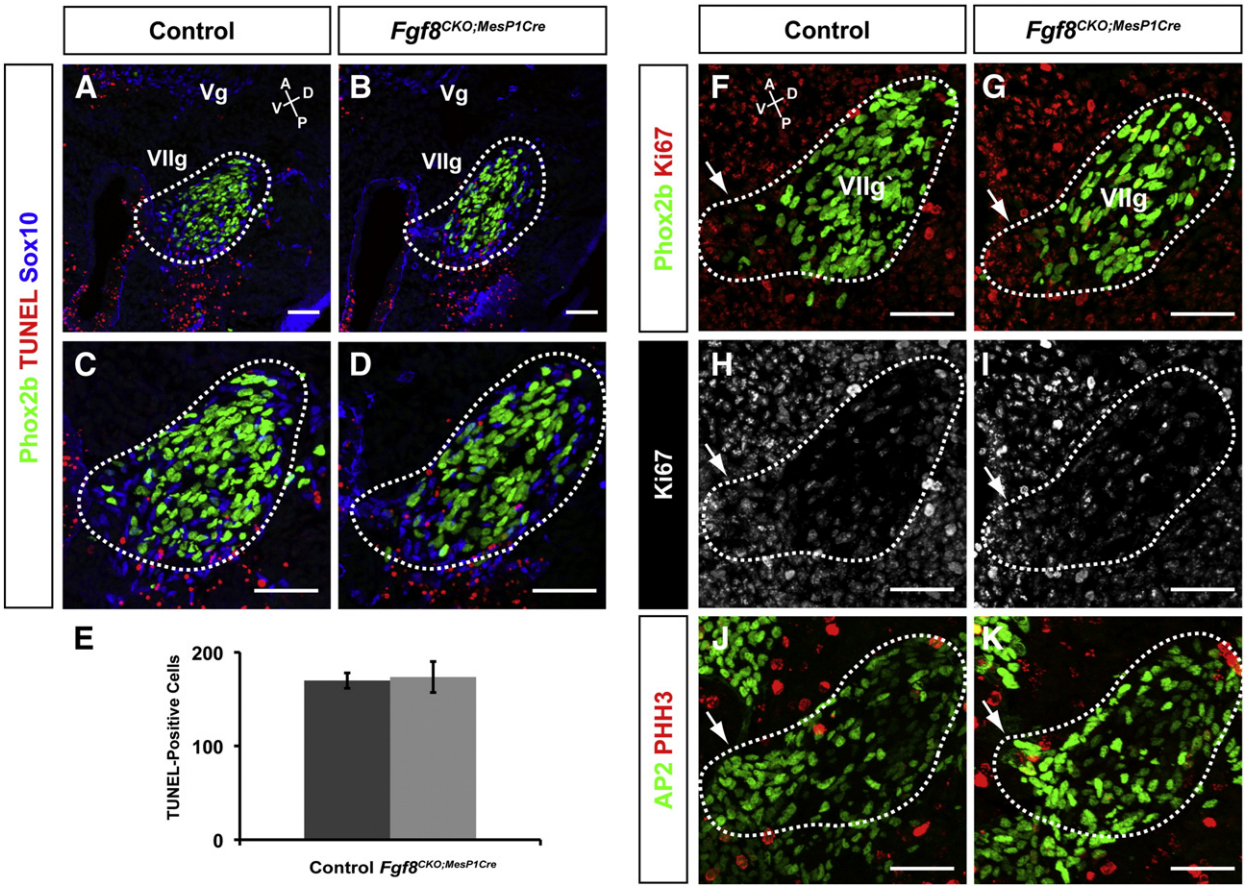

Fig. 4. Mesodermal *Fgf8* has no effect on proliferation and apoptosis of PG precursors associated with placode-derived geniculate ganglia. (A–D) Sagittal sections of e9.5 control (n = 3) and $Fgf8^{CKO};MesP1^{Cre/+}$ (n = 3) embryos through the geniculate ganglion immunolabeled for Phox2b (green) and Sox10 (blue), and assayed for TUNEL (red). Panels C and D (40X) are higher magnifications of panels A and B (20X) to better show the resolution of the immunolabeling and TUNEL staining associated with the geniculate ganglion (VIIg). (E) Quantitative analysis of TUNEL-positive grains associated with geniculate ganglion show no significant difference ($p = 0.87$) between control (n = 3) and $Fgf8^{CKO};MesP1^{Cre/+}$ (n = 3) embryos. The error bar indicate standard error mean. (F–I) Sagittal sections of e9.5 control (n = 3) and $Fgf8^{CKO};MesP1^{Cre/+}$ (n = 3) embryos through the geniculate ganglion immunolabeled for Phox2b (green) and Ki67 (red) (F, G). The channel for Ki67 was separated for clarity, and represented in panels H and I. Note the relatively low intensity and number of Ki67-expressing cells within the geniculate ganglion compared to the surrounding areas. This not only shows specificity of the staining, but also the relatively greater number of cells in S-phase in the areas surrounding the geniculate ganglion. (J–K) Sagittal sections of e9.5 control (n = 3) and $Fgf8^{CKO};MesP1^{Cre/+}$ (n = 3) embryos through the geniculate ganglion (VIIg) immunolabeled for AP2 (green) and Phospho-Histone H3 (PHH3, red). Note that the relatively fewer PHH3-expressing cells within the geniculate ganglion compared to the surrounding areas. The dotted outline circumscribes the geniculate ganglion and associated r4 neural crest stream. The arrow indicates the location where the NC-derived PG precursors emerge from the geniculate ganglion. Abbreviations: Vg, trigeminal ganglion; CKO, conditional knockout; A, anterior; P, posterior; D, dorsal; V, ventral. Scale bar = 50 μm.

that the number $Phox2b^{+}Isl1^{+}$ neurons in the geniculate ganglion were not significantly different from control littermate embryos (Fig. 6). This is consistent with the data observed for e12.5 *Fgf8* hypomorph embryos (Fig. 2L–N).

Mesodermal Fgf8 contributes to the early differentiation of PG neurons emerging from the placode-derived sensory ganglia

We have previously shown that the epibranchial placode-derived geniculate ganglion in ba2 is an intermediate migratory target of r4 NC-derived PG precursors en route to their target sites in the maxillary and mandibular arches (Takano-Maruyama et al., 2010). NC cells migrate into the geniculate ganglion with a $Sox10^{+}Phox2b^{-}$ (single-positive) molecular profile and emerge as $Sox10^{+}Phox2b^{+}$ (double-positive) PG precursors as early as e9.5. Since the NC migratory pathway between the dorsal hindbrain and the epibranchial placode-derived sensory ganglia was unaffected by elimination of mesodermal *Fgf8*, we next examined whether the migration or differentiation of PG precursors was affected at the level of the geniculate ganglion. Sagittal sections of e9.5 control and $Fgf8^{CKO}$ embryos were immunolabeled for Phox2b to define the placode-derived geniculate ganglion, and Sox10 to define the associated r4 NC cells (Figs. 7A–F; Sox10 and Phox2b are separated in panels C–F for clarity). In control embryos, the NC cells that commit to the PG lineage express Phox2b, and therefore are $Phox2b^{+}Sox10^{+}$ cells (Takano-Maruyama et al., 2010). We observed that these early NC-derived PG precursors are intercalated among the $Phox2b^{+}$-single positive sensory neurons of the placode-derived geniculate ganglion (Fig. 7A). This NC population appears to emerge from the epibranchial placode-derived geniculate ganglion, and presumably migrate rostrally as a cluster along the underlying endoderm. This cluster likely contributes to the early wave of PG precursors that migrates rostrally to become the Spg and Smg (D'Amico-Martel and Noden, 1983; Enomoto et al., 2000; Takano-Maruyama et al., 2010; Yang et al., 2008). In $Fgf8^{CKO}$ embryos, we found that the total number of $Phox2b^{+}Sox10^{+}$ NC cells associated with the placode-derived geniculate ganglion was significantly reduced compared to control littermate embryos (Fig. 7G; control, 56 ± 13; $Fgf8^{CKO}$, 25 ± 7; n = 5, $p < 0.05$).

We next analyzed specific stages of PG neuronal differentiation based on the intensity of Phox2b expression within each NC-derived $Phox2b^{+}Sox10^{+}$ cell. We used the IMARIS software to quantify the relative mean intensity of each $Phox2b^{+}Sox10^{+}$ cell. The protein intensity profile for each cell provides a highly sensitive assay to determine the stage of PG neuronal differentiation. The lower Phox2b intensity indicates an early stage of differentiation of NC cells committed to the PG

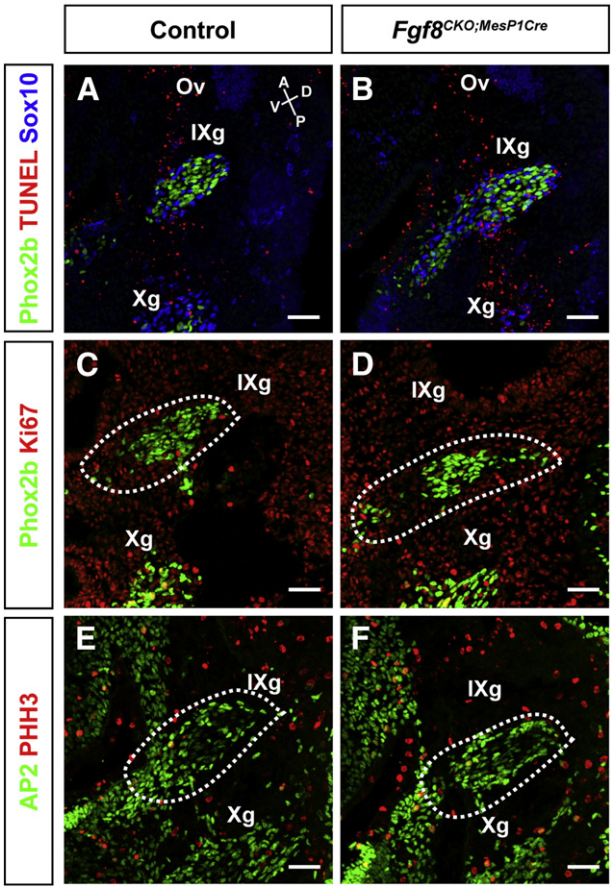

Fig. 5. Mesodermal *Fgf8* has no effect on proliferation and apoptosis of PG precursors associated with placode-derived petrosal ganglia. (A–B) Sagittal sections of e9.5 control (n = 3) and $Fgf8^{CKO};MesP1^{Cre/+}$ (n = 3) embryos through the petrosal (IXg) and nodose (Xg) ganglia immunolabeled for Phox2b (green) and Sox10 (blue), and assayed for TUNEL (red). (C–D) Sagittal sections of e9.5 control (n = 3) and $Fgf8^{CKO};MesP1^{Cre/+}$ (n = 3) embryos through the petrosal (IXg) and nodose (Xg) ganglia immunolabeled for Phox2b (green) and Ki67 (red). The dotted outline circumscribes the petrosal ganglion. (E–F) Sagittal sections of e9.5 control (n = 3) and $Fgf8^{CKO};MesP1^{Cre/+}$ (n = 3) embryos through the petrosal (IXg) and nodose (Xg) ganglia immunolabeled for AP2 (green) and Phospho-Histone H3 (PHH3, red). The dotted outline circumscribes the petrosal ganglion. Abbreviations: Ov, otic vesicle; CKO, conditional knockout; A, anterior; P, posterior; D, dorsal; V, ventral. Scale bar = 50 μm.

lineage, whereas the higher Phox2b intensity indicates a more mature stage (Chen et al., 2011; Kim et al., 2003; Takano-Maruyama et al., 2010). We then normalized single cell intensity with the total cell number, and created a relative density plot (Fig. 7H). The Phox2b mean intensity was distributed from 0 to 100 in both control (green line) and $Fgf8^{CKO}$ (red line) embryos. The relative intensity less than or equal to 50 percentile, which indicates an immature stage, was significantly greater in $Fgf8^{CKO}$ embryos compared to control littermates (Fig. 7I). In contrast, the relative intensity greater than 50 percentile, which indicates a more mature stage of differentiation, was significantly less in $Fgf8^{CKO}$ embryos compared to control littermates (Fig. 7J). In summary, the absence of mesodermal *Fgf8* resulted in fewer PG precursors, and the total population of PG precursors was at a relatively immature stage compared to controls. This suggests that mesodermal *Fgf8* contributes to the early differentiation of PG precursors at a strategic location where cranial NC cells are engaged with the epibranchial placode-derived sensory ganglia.

Discussion

The interaction of migrating NC cells with the surrounding cellular and molecular milieu is critical for the differentiation of cellular networks that are the foundation for the complex neural circuitry and structural components of the vertebrate head (Begbie and Graham, 2001; Chen et al., 2011; Coppola et al., 2010; Lumsden and Krumlauf, 1996; Mason, 2007; Shiau et al., 2008; Takano-Maruyama et al., 2010). En route to their final destination, the NC encounters cells and signaling molecules derived from all germinal layers, and the fate of the NC is thought to be determined by these factors (Bogni et al., 2008; Chen et al., 2011; Coppola et al., 2010; Kirby, 1988; Macatee et al., 2003; Nechiporuk et al., 2005; Park et al., 2008; Sato et al., 2011; Trainor and Krumlauf, 2000, 2001; Trainor et al., 2000, 2002a, 2002b). Here we used the interaction between the cranial NC the epibranchial placode as a model to understand how this cell–cell interaction is controlled at the molecular level. Specifically, we addressed how Fgf8, which is produced by multiple tissue types in the developing vertebrate head and pharynx, contributes to the regulation of this early stage of the developing cranial autonomic nervous system. We show that a global deficiency in *Fgf8* leads to a dramatic reduction of parasympathetic PG neurons of the Spg, Smg, and Og. This reduction may be due to apoptosis and/or a delay in the differentiation of NC-derived PG precursors and/or placode-derived sensory ganglia. The global reduction of *Fgf8* suggests that multiple tissue sources may regulate these processes. Indeed, we found a specific defect in the differentiation of early PG precursors by specifically eliminating mesodermal *Fgf8* in the mouse embryo. Our study has uncovered both global and tissue-specific contributions of Fgf8 during a critical stage of cranial NC-epibranchial placode interaction.

Convergence of Fgf8 from multiple tissues on the cranial neural crest

The route of the cranial NC-derived PG precursors of the Spg, Smg, and Og can be defined into two migratory streams: the ventrolateral or proximal, and the rostral or distal (Chen et al., 2011; Takano-Maruyama et al., 2010). The ventrolateral stream represents the migratory route of NC cells that span from the dorsolateral edges of r4 and r6 to the adjacent placode-derived geniculate and petrosal ganglia, respectively. Upon migrating through the placode-derived ganglia, the NC cells emerge as the rostral stream directed to various terminal target sites. Along the entire migratory pathway, Fgf8 is expressed at critical locations in tissues that arise from all germinal layers — ectoderm, mesoderm, and endoderm (Bueno et al., 1996; Ladher et al., 2005; Mason, 2007; Nechiporuk et al., 2005; Park et al., 2006; Trainor et al., 2002a). Thus, Fgf8 may affect many aspects of NC development from cell survival to migration and differentiation.

With a global reduction in *Fgf8*, we observed a significant loss of NC-derived PG neurons of the Spg, Smg, and Og in *Fgf8* hypomorphic embryos at e12.5. Although aspects of this phenotype may be the secondary consequence of extensive craniofacial defects in these mutants, we were nonetheless able to identify key components of the PG developmental pathway that contribute to the later loss of PG neurons. At e9.5, we observed massive apoptosis in the ventrolateral stream of NC cells at the level of r4 and r6 in *Fgf8* hypomorph embryos. The survival of NC cells appears to require the combined activities of Fgf8 from multiple tissues, as tissue-specific ablation of Fgf8 in either the mesoderm or ectoderm does not lead to abnormal NC apoptosis as observed in *Fgf8* hypomorph embryos. Although the phenotype in *Fgf8* hypomorph embryos contributes to the reduction of PG neurons, it is not restricted to the NC population that gives rise to PG neurons, because the NC destined for the branchial arches also undergo extensive apoptosis (Abu-Issa et al., 2002; Frank et al., 2002; Sato et al., 2011). At this point it is unclear if this is the result of direct Fgf8 signaling to the NC, or Fgf8-dependent changes in the signaling milieu or extracellular matrix. Additional studies will be required to address this question.

A second key element that likely contributes to the loss of PG neurons in *Fgf8* hypomorphs is the severe reduction of the placode-

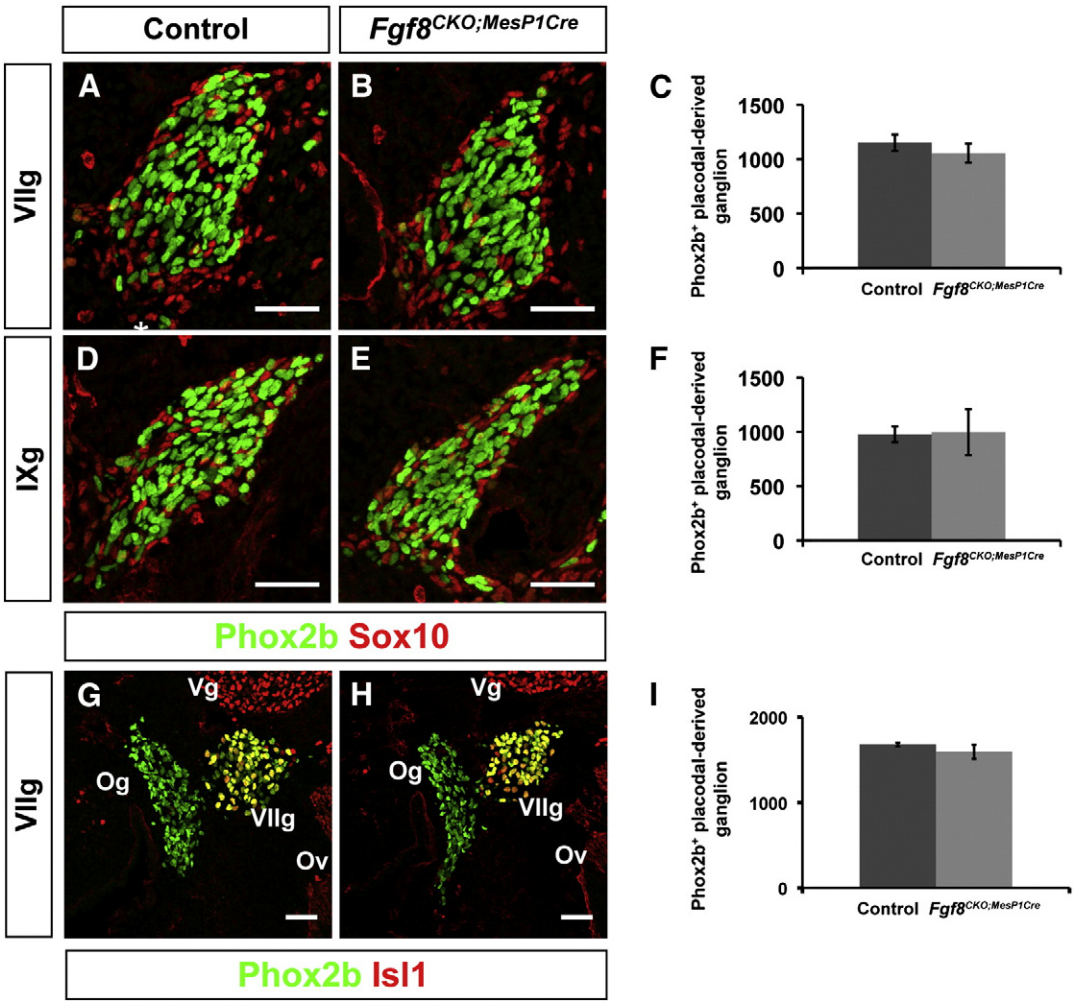

Fig. 6. Mesodermal *Fgf8* does not affect the formation of the placode-derived geniculate and petrosal ganglia. (A, B) Sagittal sections of e9.5 control (n = 3) and $Fgf8^{CKO}$;$MesP1^{Cre/+}$ (n = 3) embryos through the geniculate (VIIg) ganglion immunolabeled for Phox2b (green) and Sox10 (red). (C) The total number of $Phox2b^{+}$ neurons in the placode-derived geniculate ganglion of control and $Fgf8^{CKO}$ embryos was not statistically different ($p = 0.34$). (D, E) Sagittal sections of e9.5 control (n = 3) and $Fgf8^{CKO}$;$MesP1^{Cre/+}$ (n = 3) embryos through the petrosal (VIIg) ganglion immunolabeled Phox2b (green) and Sox10 (red). (F) The total number of $Phox2b^{+}$ neurons in the placode-derived petrosal ganglia of control and $Fgf8^{CKO}$ embryos was not statistically different $p = 0.91$). (G, H) Sagittal sections of e12.5 control (n = 3) and $Fgf8^{CKO}$;$MesP1^{Cre/+}$ (n = 3) embryos through the geniculate (VIIg) ganglion immunolabeled Phox2b (green) and Isl1 (red). (I) The total number of $Phox2b^{+}$ neurons in the epibranchial placode-derived geniculate ganglion showed no significant difference between control and $Fgf8^{CKO}$;$MesP1^{Cre/+}$ embryos (n = 2, $p = 0.4$). The error bar represents standard error mean. Abbreviations: CKO, conditional knockout V, ventral; VIIg, geniculate ganglion; Og, otic ganglion; Ov, otic vesicle. Scale bar = 50 μm.

derived geniculate and petrosal ganglia at e9.5. Others and we previously demonstrated that the loss of the epibranchial placode-derived geniculate and petrosal ganglia in *Neurog* mutant embryos was associated with apoptosis of r4 and r6 NC cells at e9.5, respectively (Chen et al., 2011; Coppola et al., 2010; Takano-Maruyama et al., 2010). This was associated with the loss of the Spg, Smg, and Og. However, the branchial arches of *Neurog* embryos were similar to that of control embryos, suggesting that the loss of the placode-derived ganglia may be specific to the NC precursors that give rise to PG neurons (Fode et al., 1998; Ma et al., 1998). The reduction of the placode-derived sensory ganglia in *Fgf8* hypomorph embryos may be a consequence of their requirement on Fgf8 production from the ectoderm or endoderm (Ladher et al., 2005; Park et al., 2006). However, our study indicates that the formation of the placode-derived geniculate and petrosal ganglia is independent of ectoderm-derived Fgf8 (Supplementary Fig. 2). It also appears that mesoderm-derived Fgf8 does not affect the formation of placode-derived ganglia. However, we cannot exclude the possibility that the formation of placode-derived ganglia may require the convergence of Fgf8 signals from both the ectoderm and mesoderm (as well as the endoderm). Evidence for this idea has been shown in zebrafish. In zebrafish, it appears that endoderm-derived Fgf3 contributes to epibranchial placodal neurogenesis, whereas the combined activities of Fgf3 and Fgf8 from the mesoderm contribute to epibranchial placodal induction (Nechiporuk et al., 2005, 2007; Sun et al., 2007). Further work to ablate Fgf8 in multiple tissues could provide insight into a possible Fgf8-tissue dose-dependent requirement for the epibranchial placodes.

Regulation of neural crest differentiation at an intermediate migratory target

Previous studies have shown that the formation of the cranial parasympathetic and visceral sensory ganglia requires the reciprocal interaction between cells derived from the NC and the epibranchial placode, respectively (Begbie and Graham, 2001; Chen et al., 2011; Coppola et al., 2010; Takano-Maruyama et al., 2010). The complex spatiotemporal expression pattern of Fgf8, and the phenotype associated with the global reduction of Fgf8 in hypomorphs indicate a broad role for Fgf8 in the developing cranial autonomic nervous system. However, evidence in zebrafish indicates that Fgf signals from the endoderm has a specific role in controlling epibranchial placode neurogenesis, which may be masked when *Fgf* is globally reduced or ablated from multiple tissues (Crump et

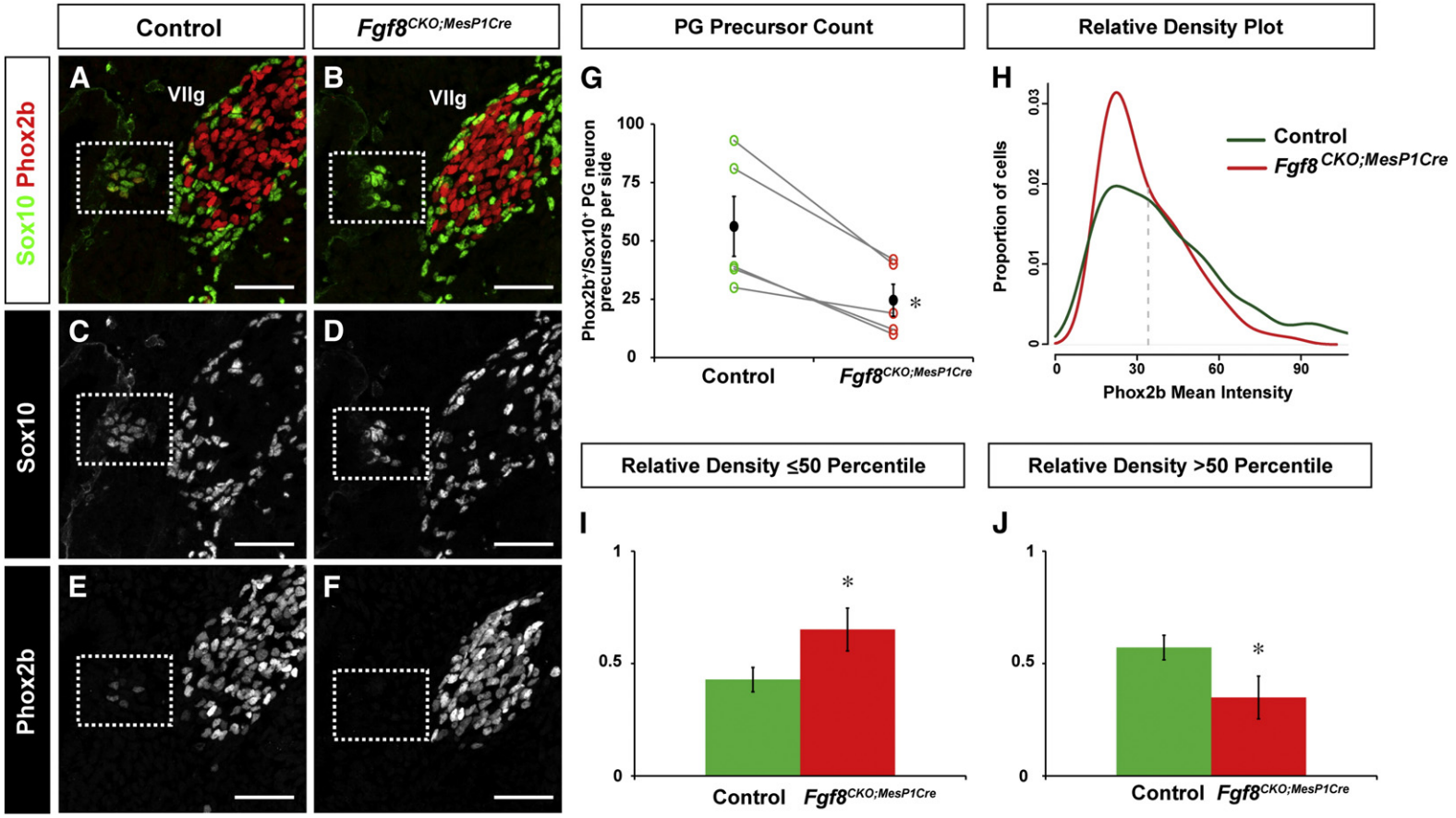

Fig. 7. Ablation of mesodermal *Fgf8* affects PG precursor number and differentiation. (A–F) Sagittal sections of e9.5 control (n = 5) and *Fgf8*^{CKO};*MesP1*$^{Cre/+}$ (n = 5) embryos through r4-derived NC cells and epibranchial placode-derived geniculate ganglion immunolabeled for Sox10 (green) and Phox2b (red). The boxes indicate the location of r4 NC-derived PG precursors emerging from the geniculate ganglion. The green and red channels in panels A and B were separated in panels C–F (black and white) to show with better clarity the relative expression levels of Sox10 and Phox2b. (G) Quantitative analysis of the total Phox2b^{+}/Sox10^{+} PG precursors per side in control (n = 5) and *Fgf8*^{CKO};*MesP1*$^{Cre/+}$ (n = 5) embryos. Each gray line shows one pair of control and *Fgf8*^{CKO};*MesP1*$^{Cre/+}$ littermate. The green and red circles indicate control and *Fgf8*^{CKO};*MesP1*$^{Cre/+}$ embryos, respectively. The black dot indicates the mean value, and the error bar indicates the standard error mean (* $p<0.05$). (H) Quantitative analysis of the relative mean intensity of Phox2b expression in the total number of PG precursors in e9.5 control and *Fgf8*^{CKO};*MesP1*$^{Cre/+}$ embryos. The mean intensity of a single PG precursor in each set was normalized to the total number. The green and red lines in the relative density plot represent the relative mean intensity distribution for control and *Fgf8*^{CKO};*MesP1*$^{Cre/+}$ embryos, respectively. The vertical gray dashed line marks the 50 percentile. (I, J) Relative density less than or equal to 50 percentile was plotted in panel I, and the relative density greater than 50 percentile was plotted in panel J. The error bar indicates the standard error mean (* $p<0.05$). Abbreviations: VIIg, geniculate ganglion; CKO, conditional knockout. Scale bar = 50 μm.

al., 2004; Mason, 2007; Nechiporuk et al., 2005; Trokovic et al., 2005). Consistent with this idea, we found a specific defect in the interaction between NC- and placode-derived neuronal precursors when *Fgf8* was conditionally ablated in the mesoderm. In contrast to the global reduction of *Fgf8* in hypomorphs, the loss of mesodermal *Fgf8* had no effect on apoptosis or in the early differentiation of placode-derived ganglia. Rather, we observed a significant reduction in the number of PG neurons that emerged from the placode-derived ganglia. Furthermore, our quantitative intensity analysis of the PG neuronal determinant Phox2b revealed that PG neurons in the mesodermal *Fgf8*-deficient embryos were immature compared to control embryos. The reduction in early PG neurons and their state of differentiation at e9.5 may therefore contribute to the overall reduction of PG neurons in the Spg, Smg, and Og in older mesodermal *Fgf8*-deficient embryos analyzed at e12.5.

The effect of mesodermal *Fgf8* reveals another level of control in the differentiation of the cranial NC fated for the PG lineage. A global reduction in Fgf8 function revealed a critical role for this protein in cell survival in the ventrolateral stream of NC cells at e9.5. The reduction and immature state of PG neurons emerging from the placode-derived ganglia suggests that mesodermal Fgf8 influences an intermediate target between the ventrolateral and rostral streams of NC cells. This intermediate target (the placode-derived sensory ganglia) contains both epibranchial placode- and NC-derived cells. Interestingly, neither the number of placode-derived neurons nor the inward migration of the placode-derived geniculate and petrosal ganglia, which is normally facilitated by NC cells (Begbie and Graham, 2001), were affected by the loss of mesodermal *Fgf8*. This suggests that the NC population that facilitates the inward migration of the placode-derived sensory ganglia may be different from the population that gives rises to PG precursors. Importantly, this suggests that the effect of mesodermal Fgf8 may be unique to the differentiation of PG neurons emerging from the placode-derived ganglia.

Our findings indicate that mesodermal *Fgf8* influences the number and differentiation of NC-derived PG precursors. The reduction and immature state of PG precursors in mesodermal *Fgf8*-deficient embryos at e9.5 suggest that Fgf8 may contribute to the regulation of the cell cycle, as previously shown for progenitors in the developing midbrain (Fischer et al., 2011). In contrast to the 80–90% reduction in PG neurons in *Fgf8* hypomorphs, the 20–30% reduction in mesodermal *Fgf8*-deficient embryos suggests a limited, but meaningful contribution of mesodermal Fgf8 in cell cycle regulation. A more thorough analysis of the cell cycle status of PG precursors during their protracted development, between e9.5-e12.5 (Takano-Maruyama et al., 2010), will be required to fully assess the contribution of Fgf8 in the duration or regulation of the cell cycle. Lastly, since the placode- and NC-derived ganglia are intact in mesodermal *Fgf8*-deficient embryos, it is unlikely that Fgf8 controls complementary molecules that are critical for the reciprocal interaction and subsequent gangliogenesis of epibranchial placode- and NC-derived neuronal precursors, as previously shown for the trigeminal ganglion (Shiau et al., 2008). Together, our study suggests that global Fgf8 coordinates the overall formation of the cranial NC- and epibranchial placode-derived cranial autonomic ganglia, but tissue-specific contributions regulate distinct aspects of cellular survival and differentiation.

Acknowledgments

We would like to thank Dr. D.J. Anderson for providing reagents, Dr. D. Ko and X. Wang for expert advice on statistics, Dr. C. Witt for imaging software, members of the NIH-SNRP-SAC for helpful comments, and O. Trevino for technical assistance. This study was supported by grants to G.O.G from the NIH (NS060658) and the Whitehall Foundation.

Appendix A. Supplementary data

Supplementary data to this article can be found online at doi:10.1016/j.ydbio.2011.10.019.

References

Abu-Issa, R., Smyth, G., Smoak, I., Yamamura, K., Meyers, E.N., 2002. Fgf8 is required for pharyngeal arch and cardiovascular development in the mouse. Development 129, 4613–4625.
Al-Hadithi, B.A., Mitchell, J., 1987. The otic ganglion and its neural connections in the rat. J. Anat. 154, 113–119.
Artinger, K.B., Fedtsova, N., Rhee, J.M., Bronner-Fraser, M., Turner, E., 1998. Placodal origin of Brn-3-expressing cranial sensory neurons. J. Neurobiol. 36, 572–585.
Baker, C.V., Bronner-Fraser, M., 2001. Vertebrate cranial placodes I. Embryonic induction. Dev. Biol. 232, 1–61.
Baker, C.V., Stark, M.R., Marcelle, C., Bronner-Fraser, M., 1999. Competence, specification and induction of Pax-3 in the trigeminal placode. Development 126, 147–156.
Begbie, J., Ballivet, M., Graham, A., 2002. Early steps in the production of sensory neurons by the neurogenic placodes. Mol. Cell. Neurosci. 21, 502–511.
Begbie, J., Brunet, J.F., Rubenstein, J.L., Graham, A., 1999. Induction of the epibranchial placodes. Development 126, 895–902.
Begbie, J., Graham, A., 2001. Integration between the epibranchial placodes and the hindbrain. Science 294, 595–598.
Bogni, S., Trainor, P., Natarajan, D., Krumlauf, R., Pachnis, V., 2008. Non-cell-autonomous effects of Ret deletion in early enteric neurogenesis. Development 135, 3007–3011.
Bueno, D., Skinner, J., Abud, H., Heath, J.K., 1996. Spatial and temporal relationships between Shh, Fgf4, and Fgf8 gene expression at diverse signalling centers during mouse development. Dev. Dyn. 207, 291–299.
Chen, Y., Takano-Maruyama, M., Gaufo, G.O., 2011. Plasticity of neural crest-placode interaction in the developing visceral nervous system. Dev. Dyn. 240, 1880–1888.
Coppola, E., Rallu, M., Richard, J., Dufour, S., Riethmacher, D., Guillemot, F., Goridis, C., Brunet, J.F., 2010. Epibranchial ganglia orchestrate the development of the cranial neurogenic crest. Proc. Natl. Acad. Sci. U. S. A. 107, 2066–2071.
Creuzet, S., Couly, G., Le Douarin, N.M., 2005. Patterning the neural crest derivatives during development of the vertebrate head: insights from avian studies. J. Anat. 207, 447–459.
Crump, J.G., Maves, L., Lawson, N.D., Weinstein, B.M., Kimmel, C.B., 2004. An essential role for Fgfs in endodermal pouch formation influences later craniofacial skeletal patterning. Development 131, 5703–5716.
D'Amico-Martel, A., Noden, D.M., 1983. Contributions of placodal and neural crest cells to avian cranial peripheral ganglia. Am. J. Anat. 166, 445–468.
Enomoto, H., Araki, T., Jackman, A., Heuckeroth, R.O., Snider, W.D., Johnson Jr., E.M., Milbrandt, J., 1998. GFR alpha1-deficient mice have deficits in the enteric nervous system and kidneys. Neuron 21, 317–324.
Enomoto, H., Heuckeroth, R.O., Golden, J.P., Johnson, E.M., Milbrandt, J., 2000. Development of cranial parasympathetic ganglia requires sequential actions of GDNF and neurturin. Development 127, 4877–4889.
Fischer, T., Faus-Kessler, T., Welzl, G., Simeone, A., Wurst, W., Prakash, N., 2011. Fgf15-mediated control of neurogenic and proneural gene expression regulates dorsal midbrain neurogenesis. Dev. Biol. 350, 496–510.
Fode, C., Gradwohl, G., Morin, X., Dierich, A., LeMeur, M., Goridis, C., Guillemot, F., 1998. The bHLH protein NEUROGENIN 2 is a determination factor for epibranchial placode-derived sensory neurons. Neuron 20, 483–494.
Frank, D.U., Fotheringham, L.K., Brewer, J.A., Muglia, L.J., Tristani-Firouzi, M., Capecchi, M.R., Moon, A.M., 2002. An Fgf8 mouse mutant phenocopies human 22q11 deletion syndrome. Development 129, 4591–4603.
Gammill, L.S., Gonzalez, C., Bronner-Fraser, M., 2007. Neuropilin 2/semaphorin 3F signaling is essential for cranial neural crest migration and trigeminal ganglion condensation. Dev. Neurobiol. 67, 47–56.
Gammill, L.S., Gonzalez, C., Gu, C., Bronner-Fraser, M., 2006. Guidance of trunk neural crest migration requires neuropilin 2/semaphorin 3F signaling. Development 133, 99–106.
Hamburger, V., 1961. Experimental analysis of the dual origin of the trigeminal ganglion in the chick embryo. J. Exp. Zool. 148, 91–123.
Heuckeroth, R.O., Enomoto, H., Grider, J.R., Golden, J.P., Hanke, J.A., Jackman, A., Molliver, D.C., Bardgett, M.E., Snider, W.D., Johnson Jr., E.M., Milbrandt, J., 1999. Gene targeting reveals a critical role for neurturin in the development and maintenance of enteric, sensory, and parasympathetic neurons. Neuron 22, 253–263.
Jaskoll, T., Abichaker, G., Witcher, D., Sala, F.G., Bellusci, S., Hajihosseini, M.K., Melnick, M., 2005. FGF10/FGFR2b signaling plays essential roles during in vivo embryonic submandibular salivary gland morphogenesis. BMC Dev. Biol. 5, 11.
Jaskoll, T., Witcher, D., Toreno, L., Bringas, P., Moon, A.M., Melnick, M., 2004. FGF8 dose-dependent regulation of embryonic submandibular salivary gland morphogenesis. Dev. Biol. 268, 457–469.
Kandel, E.R., Schwartz, J.H., Jessell, T.M., 2000. Principles of Neural Science, 4th ed. McGraw-Hill, Health Professions Division, New York.
Kim, J., Lo, L., Dormand, E., Anderson, D.J., 2003. SOX10 maintains multipotency and inhibits neuronal differentiation of neural crest stem cells. Neuron 38, 17–31.
Kirby, M.L., 1988. Nodose placode contributes autonomic neurons to the heart in the absence of cardiac neural crest. J. Neurosci. 8, 1089–1095.
Ladher, R.K., Wright, T.J., Moon, A.M., Mansour, S.L., Schoenwolf, G.C., 2005. FGF8 initiates inner ear induction in chick and mouse. Genes Dev. 19, 603–613.
Le Douarin, N.M., Creuzet, S., Couly, G., Dupin, E., 2004. Neural crest cell plasticity and its limits. Development 131, 4637–4650.
Lumsden, A., Krumlauf, R., 1996. Patterning the vertebrate neuraxis. Science 274, 1109–1115.
Lumsden, A., Sprawson, N., Graham, A., 1991. Segmental origin and migration of neural crest cells in the hindbrain region of the chick embryo. Development 113, 1281–1291.
Ma, Q., Chen, Z., del Barco Barrantes, I., de la Pompa, J.L., Anderson, D.J., 1998. Neurogenin1 is essential for the determination of neuronal precursors for proximal cranial sensory ganglia. Neuron 20, 469–482.

Macatee, T.L., Hammond, B.P., Arenkiel, B.R., Francis, L., Frank, D.U., Moon, A.M., 2003. Ablation of specific expression domains reveals discrete functions of ectoderm- and endoderm-derived FGF8 during cardiovascular and pharyngeal development. Development 130, 6361–6374.

Mason, I., 2007. Initiation to end point: the multiple roles of fibroblast growth factors in neural development. Nat. Rev. Neurosci. 8, 583–596.

McCabe, K.L., Bronner-Fraser, M., 2008. Essential role for PDGF signaling in ophthalmic trigeminal placode induction. Development 135, 1863–1874.

Monsoro-Burq, A.H., Wang, E., Harland, R., 2005. Msx1 and Pax3 cooperate to mediate FGF8 and WNT signals during Xenopus neural crest induction. Dev. Cell 8, 167–178.

Moon, A.M., Capecchi, M.R., 2000. Fgf8 is required for outgrowth and patterning of the limbs. Nat. Genet. 26, 455–459.

Nechiporuk, A., Linbo, T., Poss, K.D., Raible, D.W., 2007. Specification of epibranchial placodes in zebrafish. Development 134, 611–623.

Nechiporuk, A., Linbo, T., Raible, D.W., 2005. Endoderm-derived Fgf3 is necessary and sufficient for inducing neurogenesis in the epibranchial placodes in zebrafish. Development 132, 3717–3730.

Noden, D.M., Trainor, P.A., 2005. Relations and interactions between cranial mesoderm and neural crest populations. J. Anat. 207, 575–601.

Park, E.J., Ogden, L.A., Talbot, A., Evans, S., Cai, C.L., Black, B.L., Frank, D.U., Moon, A.M., 2006. Required, tissue-specific roles for Fgf8 in outflow tract formation and remodeling. Development 133, 2419–2433.

Park, E.J., Watanabe, Y., Smyth, G., Miyagawa-Tomita, S., Meyers, E., Klingensmith, J., Camenisch, T., Buckingham, M., Moon, A.M., 2008. An FGF autocrine loop initiated in second heart field mesoderm regulates morphogenesis at the arterial pole of the heart. Development 135, 3599–3610.

Pattyn, A., Morin, X., Cremer, H., Goridis, C., Brunet, J.F., 1999. The homeobox gene Phox2b is essential for the development of autonomic neural crest derivatives. Nature 399, 366–370.

Saga, Y., Hata, N., Kobayashi, S., Magnuson, T., Seldin, M.F., Taketo, M.M., 1996. MesP1: a novel basic helix-loop-helix protein expressed in the nascent mesodermal cells during mouse gastrulation. Development 122, 2769–2778.

Sato, A., Scholl, A.M., Kuhn, E.B., Stadt, H.A., Decker, J.R., Pegram, K., Hutson, M.R., Kirby, M.L., 2011. FGF8 signaling is chemotactic for cardiac neural crest cells. Dev. Biol. 354, 18–30.

Schlosser, G., 2010. Making senses development of vertebrate cranial placodes. Int. Rev. Cell Mol. Biol. 283, 129–234.

Schwarz, Q., Vieira, J.M., Howard, B., Eickholt, B.J., Ruhrberg, C., 2008. Neuropilin 1 and 2 control cranial gangliogenesis and axon guidance through neural crest cells. Development 135, 1605–1613.

Shiau, C.E., Bronner-Fraser, M., 2009. N-cadherin acts in concert with Slit1-Robo2 signaling in regulating aggregation of placode-derived cranial sensory neurons. Development 136, 4155–4164.

Shiau, C.E., Lwigale, P.Y., Das, R.M., Wilson, S.A., Bronner-Fraser, M., 2008. Robo2-Slit1 dependent cell–cell interactions mediate assembly of the trigeminal ganglion. Nat. Neurosci. 11, 269–276.

Stark, M.R., Sechrist, J., Bronner-Fraser, M., Marcelle, C., 1997. Neural tube-ectoderm interactions are required for trigeminal placode formation. Development 124, 4287–4295.

Sun, S.K., Dee, C.T., Tripathi, V.B., Rengifo, A., Hirst, C.S., Scotting, P.J., 2007. Epibranchial and otic placodes are induced by a common Fgf signal, but their subsequent development is independent. Dev. Biol. 303, 675–686.

Takano-Maruyama, M., Chen, Y., Gaufo, G.O., 2010. Placodal sensory ganglia coordinate the formation of the cranial visceral motor pathway. Dev. Dyn. 239, 1155–1161.

Trainor, P.A., Ariza-McNaughton, L., Krumlauf, R., 2002a. Role of the isthmus and FGFs in resolving the paradox of neural crest plasticity and prepatterning. Science 295, 1288–1291.

Trainor, P.A., Krumlauf, R., 2000. Patterning the cranial neural crest: hindbrain segmentation and Hox gene plasticity. Nat. Rev. Neurosci. 1, 116–124.

Trainor, P.A., Krumlauf, R., 2001. Hox genes, neural crest cells and branchial arch patterning. Curr. Opin. Cell Biol. 13, 698–705.

Trainor, P.A., Manzanares, M., Krumlauf, R., 2000. Genetic interactions during hindbrain segmentation in the mouse embryo. Results Probl. Cell Differ. 30, 51–89.

Trainor, P.A., Sobieszczuk, D., Wilkinson, D., Krumlauf, R., 2002b. Signalling between the hindbrain and paraxial tissues dictates neural crest migration pathways. Development 129, 433–442.

Trokovic, N., Trokovic, R., Partanen, J., 2005. Fibroblast growth factor signalling and regional specification of the pharyngeal ectoderm. Int. J. Dev. Biol. 49, 797–805.

Trumpp, A., Depew, M.J., Rubenstein, J.L., Bishop, J.M., Martin, G.R., 1999. Cre-mediated gene inactivation demonstrates that FGF8 is required for cell survival and patterning of the first branchial arch. Genes Dev. 13, 3136–3148.

Uesaka, T., Jain, S., Yonemura, S., Uchiyama, Y., Milbrandt, J., Enomoto, H., 2007. Conditional ablation of GFRalpha1 in postmigratory enteric neurons triggers unconventional neuronal death in the colon and causes a Hirschsprung's disease phenotype. Development 134, 2171–2181.

Watanabe, Y., Miyagawa-Tomita, S., Vincent, S.D., Kelly, R.G., Moon, A.M., Buckingham, M.E., 2010. Role of mesodermal FGF8 and FGF10 overlaps in the development of the arterial pole of the heart and pharyngeal arch arteries. Circ. Res. 106, 495–503.

Yan, H., Bergner, A.J., Enomoto, H., Milbrandt, J., Newgreen, D.F., Young, H.M., 2004. Neural cells in the esophagus respond to glial cell line-derived neurotrophic factor and neurturin, and are RET-dependent. Dev. Biol. 272, 118–133.

Yang, X., Zhou, Y., Barcarse, E.A., O'Gorman, S., 2008. Altered neuronal lineages in the facial ganglia of Hoxa2 mutant mice. Dev. Biol. 314, 171–188.

Young, H.M., Bergner, A.J., Anderson, R.B., Enomoto, H., Milbrandt, J., Newgreen, D.F., Whitington, P.M., 2004. Dynamics of neural crest-derived cell migration in the embryonic mouse gut. Dev. Biol. 270, 455–473.

Yu, S., Poe, B., Schwarz, M., Elliot, S.A., Albertine, K.H., Fenton, S., Garg, V., Moon, A.M., 2010. Fetal and postnatal lung defects reveal a novel and required role for Fgf8 in lung development. Dev. Biol. 347, 92–108.